INTERNATIONAL JOURNAL OF PRECISION ENGINEERING AND MANUFACTURING Vol. 15, No. 10, pp. 2141-2147 OCTOBER 2014 / 2141
DOI: 10.1007/s12541-014-0574-8

Novel Piezo Driven Motion Amplified Stage

Ho Je Jung[1] and Jung Hyun Kim[1,#]

1 Department of Mechatronics, Kyung Sung University, 314-79, Daeyeon3-dong, Nam-gu, Busan, South Korea, 608-736
Corresponding Author / E-mail: dwellnom@ks.ac.kr, TEL: +82-51-663-4694, FAX: +82-51-626-4773

KEYWORDS: Compliant mechanism, Micro-motion stage, Piezoelectric actuator

This paper presents a novel piezo driven motion stage employing multiple motion levers allowing for an amplification ratio that exceeds 60x enabled by a newly contrived cross hinge structure. Optimization of the motion stage was performed and simulation results proved the superiority of the newly devised cross hinge compared to the conventional flexure hinge. Measurements of the motion stage were made using an optical microscope. The motion stage was incorporated into a visually served close loop motion control scheme and experimental results prove that the feedback system is capable of 20 nm nano-stepping.

Manuscript received: July 25, 2013 / Revised: June 20, 2014 / Accepted: June 23, 2014

1. Introduction

Manufacturing technology has greatly advanced in terms of being able to fabricate, manipulate and assemble materials and parts down to the nanometer scale and beyond. Especially in the area of semiconductor manufacturing, these advancements have enabled manufacturers two produce products which are lighter, smarter, more energy efficient than ever before. Furthermore, high precision manufacturing is gaining ever more importance in areas such as medical devices, scientific instruments, aerospace, etc. Precision motion control is a ubiquitous and essential element in precision manufacturing where advancements in its performance and affordability can have a broad impact on manufacturing as a whole.

High precision motion control often requires precision and accuracy beyond micrometer and even in the nanometer range. In industrial settings typical motion control requirements are met by means of hydraulic/pneumatic actuators, electric motors, linear stages and etc. These methods have difficulty in implementing high precision motion control in the micrometer range due to factors such as friction, heat, stick-slip, erosion and more.

Piezoelectric elements have many advantages for implementing high precision motion: Motion resolution of nanometer and beyond can be achieved, thermal sensitivity is small, does not generate any magnetic field and the response is quick and smooth. Despite of all of its advantages piezoelectric elements have one major disadvantage in that the motion range is limited to approximately 0.1% of its length.

In order to overcome this disadvantage, longer piezoelectric elements can be used however this would significantly increase size and cost. Instead flexible motion amplifying structures can be employed which simply amplify the motion of the piezo element by taking advantage of the leverage effect. By using multiple levers the amplification of the device can be increased significantly, however in practice, the ultimate amplification is limited by the increasing stress especially in the hinges that ground and connect the levers (Fig. 1). The goal of this paper is to develop an amplification stage which employs a novel hinge design that causes less stress than prior hinges ultimately rendering a motion stage having large motion and high precision.

Previously, many motion amplification stages have been developed: Scire et al.[1] developed a single axis motion stage with 50 um range, Choi et al.[2] developed a stage with multi-flexure-hinges, Kang[3] uses a parallel lever structure to mitigate the effects of manufacturing errors, Gao et al.[4] designed a 2-axis stage that has a range of 40×40 um, Lu et al.[5] developed a 3-axis stage that is actuated by 3 piezo elements that maneuver in a parallel structure, Ryu et al.'s[6] stage employs a double compound lever to reduce loss of amplification, Hu et al.[7] developed a 6-axis stage using a bridge amplifier to change motion direction.

A common factor for almost all of these stages is that although levers were used for motion amplification only two were used at most and the hinges used were flexure hinges (Fig. 2). This is due to the fact that increasing the number of levers will increase the maximum stress occurring at the hinges and make the overall stiffness of the stage too large for the piezoelectric element to handle.

This paper introduces an amplification stage design employing a novel hinge design called the cross hinge which is more flexible and efficient than the flexure hinge. The use of this hinge allows for stacking of three levers rendering a motion amplification of ×60 which

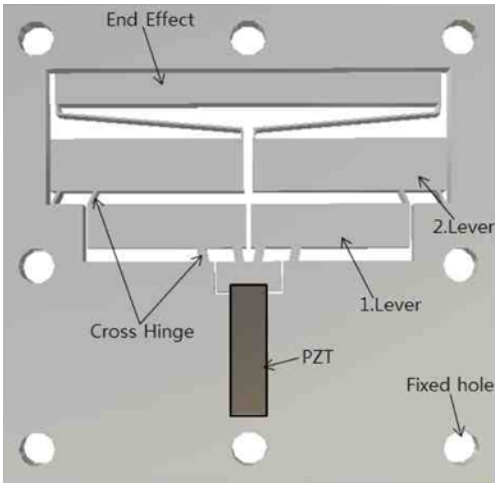

Fig. 1 Catia 3D motion stage design

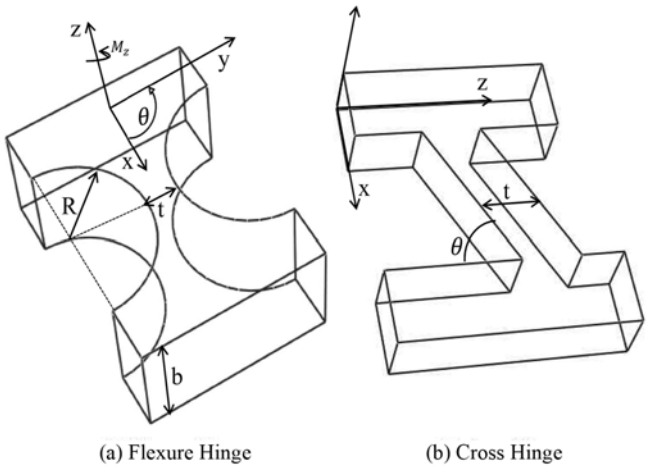

Fig. 2 Flexure hinge and Cross hinge

is much larger than previously proposed designs that have a similar structure[2] while the motion accuracy is maintained at a comparable level. Chapter 2 presents the design principle of the amplification stage and the optimization of the design and Chapter 3 presents the PID control and the experimental results.

2. Motion Stage Structure and Characteristics

2.1 Mechanical structure of stage

Fig. 1 shows a 3D CAD rendition of the motion stage. The stage is made of aluminum (Al 7075) and the size of the stage is 110 mm × 110 mm with 8 mm thickness. As shown in Table 1, the piezo element is PSt-HD200/77/40 (Piezomechanik GmbH), the size of the piezo element is 7 mm × 7 mm × 30 mm with motion range of 40 um. The stage shown in Fig. 1 employs a parallel structure placing the leverages in a symmetric formation with respect to the piezo element. This type of structure has been shown to improve both precision and linearity of motion. The stage has also been designed to accommodate monolithic fabrication allowing for convenient and economic manufacturing without any additional assembly process.

Table 1 Piezo specification

Stroke	Resonance frequency	Strength	Blocking Force
40 μm	33 KHz	40 N/μm	2500 N

In order to gain a large amplification of motion, many stage designs stack multiple levers as shown in Fig. 1. However, there are practically no instances where 3 or more levers are used due to excessive stress concentration at the motion hinges. In order to obtain higher amplification ratios with lower stress concentration at the hinges, instead of the widely used flexure hinges (Fig. 2) new designed hinges called cross hinges were employed on hinges attached to lever 1 & 2 in Fig. 1. Furthermore, the hinge connecting lever 2 and the end effector was designed to decrease stress concentration while increase motion range.

2.2 Cross hinge and flexure hinge

Fig. 2(a) and (b) respectively show diagrams of flexure and Cross hinges. Previous work almost exclusively uses flexure hinges which have a symmetric structure with rounded corners and a slim center *t* (Fig. 2). This design is intended to render low resistance against bending while having larger resistance from loads along the hinges' main axis. The rounding of corners is of course a classic method used in mechanics for the purpose of releiving stress concentration. However, when multiple levers are stacked using this type of hinge in order to create larger motions, the resistance of the hinges must be reduced which requires reducing thickness *t*. This in turn however, increases the stress concentration to unsustainable levels. The maximum stress and the maximum rotational motion of the flexure hinge can be expressed as below,

$$\sigma_{max} = \frac{6M_z K_t}{t^2 b} \tag{1}$$

$$\theta_{max} = \frac{4K}{K_t}\frac{R}{Et}\sigma_{max} \tag{2}$$

M_z is the axial moment, K_t is the stress concentration factor. From (1), one can see that t has a critical effect on the maximum stress. Also from (2), it is evident that the maximum stress is proportional to the maximum angular displacement. When large motion amplification is required, large angular displacement occurs which entails increased stress. In order to decrease the stress concentration, the most effective action is to increase thickness t, however when t is excessively increased the flexibility of the flexure hinge decreases to a point rendering it useless as a motion component. In order to overcome this issue, the authors of this paper have contrived a new hinge design.

Fig. 3(a) presents the cross section of the lever and cross hinge and Fig. 3(b) shows pure bending of the cross hinge. As shown in Fig. 2, the cross hinge is tilted in the direction adjacent to the direction of the motion vector of the lever. This has the effect increasing the length of the hinge so that it is larger than h (Fig. 3(a)), i.e., the space between two levers. This in turn has the effect of decreasing the stress concentration. Relationship between the parameters is derived below.

$$L = p\theta, \quad \theta = \theta_b - \theta_a \tag{3}$$

$$\frac{1}{p} = \frac{\theta}{L} \tag{4}$$

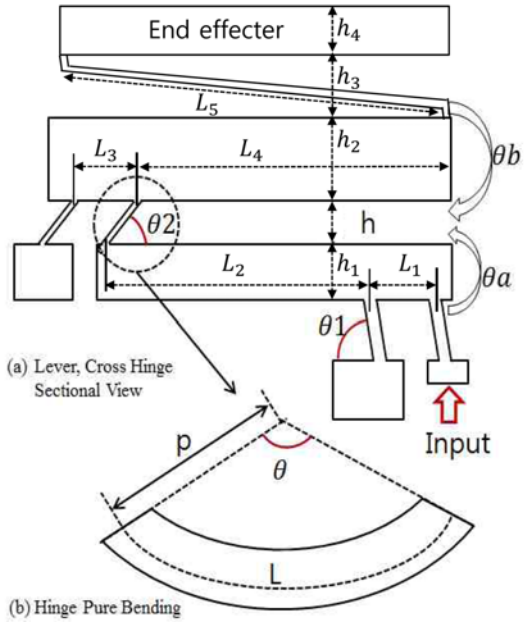

Fig. 3 Pure bending of cross hinge

Table 2 Architectural parameters

	Value		Value		Value
L_1	5.9 mm	L_5	41 mm	θ_1	80.2°
L_2	30.12 mm	h	3 mm	θ_2	50°
L_3	5.9 mm	h_1	10 mm	h_3	8 mm
L_4	34.36 mm	h_2	12 mm	h_4	7 mm

Curvature is the inverse of the bending radius,

$$\frac{1}{p} = \frac{M}{EI} \tag{5}$$

Insert (5) into (4),

$$M = \frac{EI\theta}{L} \tag{6}$$

$$\sigma_{max} = \frac{Mc}{I} \tag{7}$$

Insert (7) into (6),

$$\sigma_{max} = \frac{Ec\theta}{L} \tag{8}$$

As can be seen in the above equation, σ_{max} inverse proportional to L, so the larger L is the smaller σ_{max} becomes. As can be seen, increasingly tilting the hinge has the effect of decreasing the stress However, increasing the length extensively will have an ill effect of decreasing the amplification ratio of the lever.

The next section covers utilizing optimal design techniques to design the hinge and the entire motion stage.

2.3 Design optimization

The ansys optimization tool Goal Driven Optimization (GDO) was used for design optimization. GDO is a multipurpose optimization tool that finds the optimized design from the user defined design parameters.

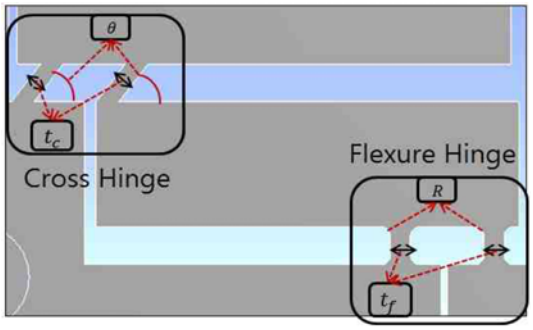

Fig. 4 Input variables

The user defines the range or values of the input and output parameters, sets weights on each of the parameters, and the tool outputs several sample designs from which the user finally selects the final design.

The purpose of this section is twofold. First, to compare the performance of the conventional flexure hinge vs the newly contrived cross hinge. Second, is to determine the final optimal design of the motion stage. In order to achieve this task, the input variables for the optimization process were chosen as seen in Fig. 4 for both Cross and Flexure Hinge respectively. For the cross hinge tilt angle θ and hinge thickness t_c were chosen. For the flexure hinge, hinge thickness t_f and rounding radius R were chosen as optimization input parameters.

The output parameters of the optimization process were chosen as follows: minimize equivalent stress and maximize end effecter motion. Flexure Hinge input parameters have the following restrictions:

$$\begin{gathered} t_f(Hinge\ 1) > t_f(Hinge\ 2) \\ R(Hinge\ 2) \le R(Hinge\ 1) \le \frac{h}{2} \\ 0.5\ \text{mm} \le t_f(Hinge\ 2) < t_f(Hinge\ 1) \\ 0.5\ \text{mm} \le R(Hinge\ 2) \le R(Hinge\ 1) \end{gathered} \tag{9}$$

Cross Hinge input parameters have the following restrictions:

$$\begin{gathered} t_c(Hinge\ 1) > t_c(Hinge\ 2) \\ \theta(Hinge\ 2) < \theta(Hinge\ 1) \le 90° \\ 0.5\ \text{mm} \le t_c(Hinge\ 2) < t_c(Hinge\ 1) \\ 50° \le \theta(Hinge\ 2) < \theta(Hinge\ 1) \end{gathered} \tag{10}$$

Since *Hinge 1* receives more force the piezo element, the thickness in that hinge must be larger than that of *Hinge 2*. Also the motion of *Hinge 1* is always smaller than that of *Hinge 2*. 0.5 mm in (9) is the minimum fabrication limit and 50° is given by the dimensions of the motion stage.

Fig. 5 presents 4 combinations of using Cross Hinge and/or Flexure Hinges for levers 1 or 2, i.e., (a) Flexure (*Hinge 1*) - Flexure (*Hinge 2*) (b) Flexure (*Hinge 1*) - Cross (*Hinge 2*) (c) Cross (*Hinge 1*) - Flexure (*Hinge 2*) (d) Cross (*Hinge 1*) - Cross (*Hinge 2*). Optimization has been performed for each 4 cases to determine which combination proves best in terms of end effecter displacement and equivalent stress.

Table 3 shows the optimization results for all 4 cases presented in Fig. 5 for end effecter displacement, equivalent stress and amplification ratio. Amplification ratio refers to the end effecter displacement divided by the 40 um input motion generated from the piezo-electric element. Fig. 6 shows the simulation result for the case where cross hinges were

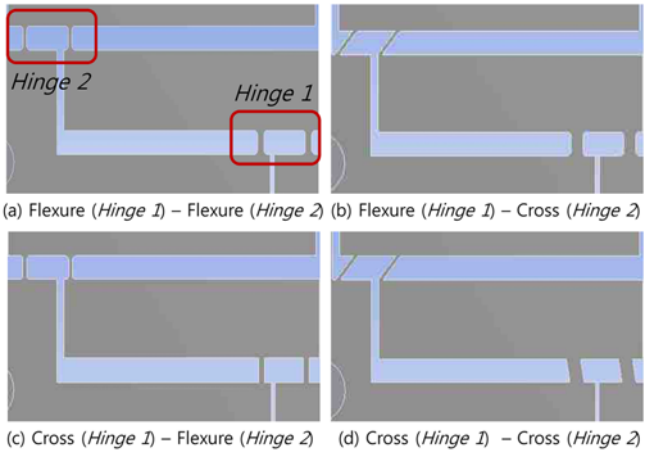

Fig. 5 Four cases of ansys optimization

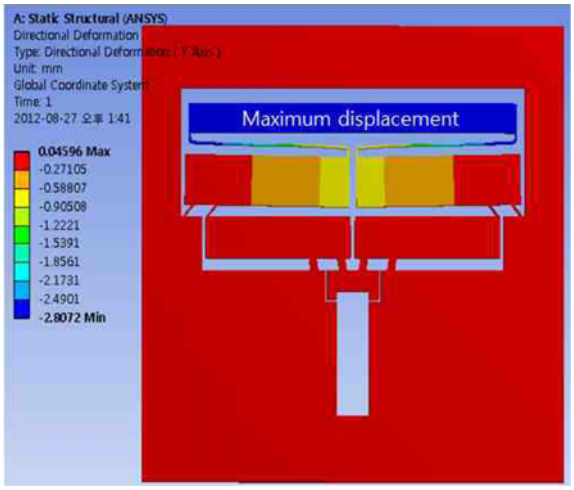

Fig. 6 End effector displacement

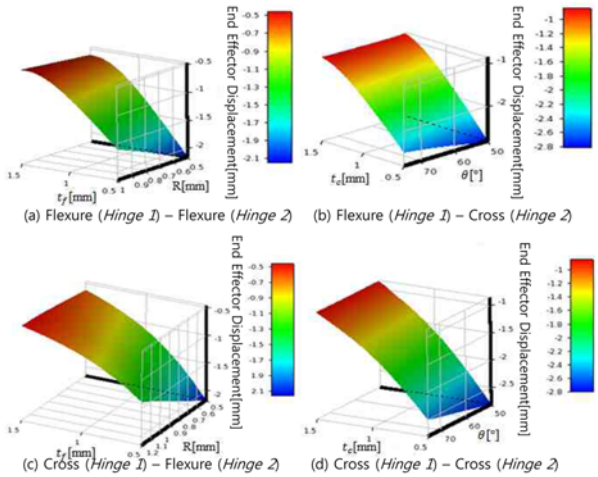

Fig. 7 End effector displacement 3D response chart

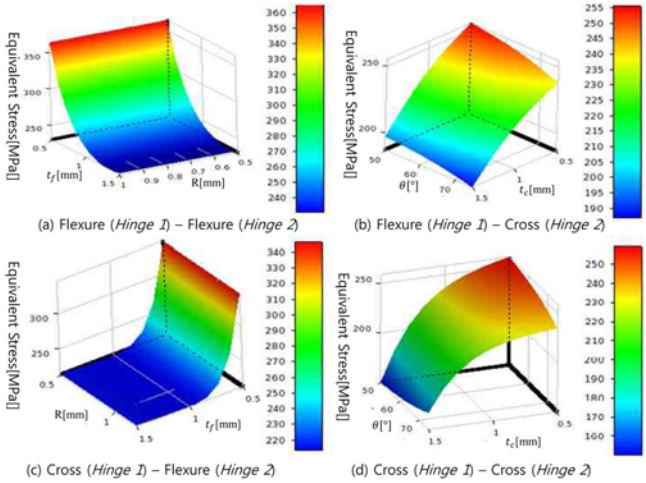

Fig. 8 Equivalent stress 3D response chart

Table 3 Optimization results

	End Effector Displacement (mm)	Equivalent Stress (MPa)	Amplification ratio
(a)	2.1422	359.21	53.555
(b)	2.8041	268.8	70.1025
(c)	2.0749	337.48	51.8725
(d)	2.8072	263.55	70.18

used for both Hinge 1 and Hinge 2.

It is evident from Table 3 that case (d) which uses cross hinges for both levers shows the best result in terms of amplification ratio and equivalent stress. Note that each case, i.e., from (a) to (d), was optimized, therefore proves that cross hinges have superior performance compared to flexure hinges.

Fig. 7 shows the relationship between the input parameters and the resulting end effecter displacement. It can be seen that when t_f and R get close to 0.5 mm the end effecter displacement gets larger and for the cross hinge, when input parameter t_c gets close to 0.5 mm and θ gets close to 0.5 mm and θ gets close to 50° the end effecter displacement gets larger. However, at the same time as the dimensions get closer to 0.5 mm, i.e., when the hinges get thinner. Fig. 8 shows the relationship between the input parameters and Equivalent Stress. It shows that the R value of the Flexure Hinge has negligible effect on the stress and with only t_f having an effect. The closer t_f gets to 1.5 mm the smaller the stress. For the cross hinge, the closer t_c gets to 1.5 mm the smaller the stress. It can be seen from Fig. 9 that maximum equivalent stress becomes larger. Therein lays the compromise that has to be weighed and decided.

The effect of cross hinge can be seen by examining the simulation result of Table 3, i.e., comparing (c) and (d) of Table 3, both have the same type of hinge at Hinge 1 but different types at Hinge 2. Result of (d) which has a cross hinge at Hinge 2 has much better performance than (c) which has a Flexure Hinge at Hinge 2. This proves the superior performance of cross hinges.

Also if you cross examine case (b) and (d), which have the same a type of hinge at Hinge 2 but different type at Hinge 1, the results barely differ at all. If you consider that the deflection is small at Hinge 1 and large at Hinge 2, this shows that cross hinges are very is effective when the deflection is large, however when the deflection small the difference

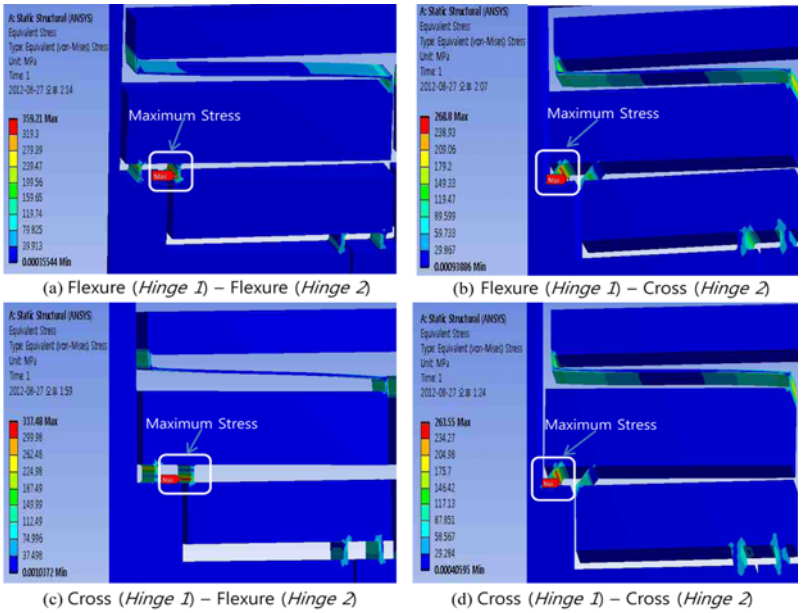

(a) Flexure (*Hinge 1*) – Flexure (*Hinge 2*) (b) Flexure (*Hinge 1*) – Cross (*Hinge 2*)

(c) Cross (*Hinge 1*) – Flexure (*Hinge 2*) (d) Cross (*Hinge 1*) – Cross (*Hinge 2*)

Fig. 9 Maximum equivalent stress occurring at Hinge 2

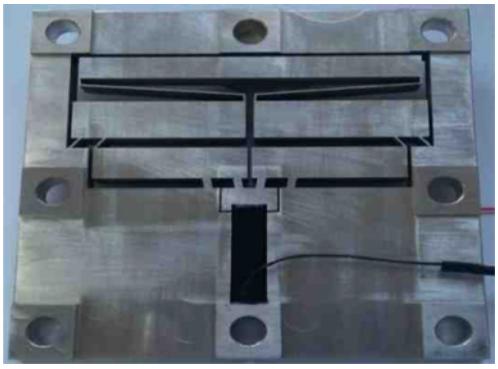

Fig. 10 Motion stage

between using a flexure or cross hinge is negligible. On the basis of this analysis, we have chosen case (d), i.e., both hinge 1 & 2 have cross hinges, as the optimal design.

3. Fabrication and Testing of Motion Stage

3.1 Motion stage fabrication

Based on the design optimization a motion stage has been fabricated as shown in Fig. 10. Aluminum (Al 7075) was selected as the choice of material for its high strength. The fabrication of the stage was a two step process: i) First was the milling process which machined the outline and surface dimensions along with the through holes, ii) Then wire electric discharge machining was applied to fabricate the fine dimensions of the motion stage.

3.2 Motion measurement

In order to measure and verify the performance of the motion stage, an optical microscope has been used as shown in Fig. 11. The optical microscope is a Leica DMLM microscope. The motion of the stage is

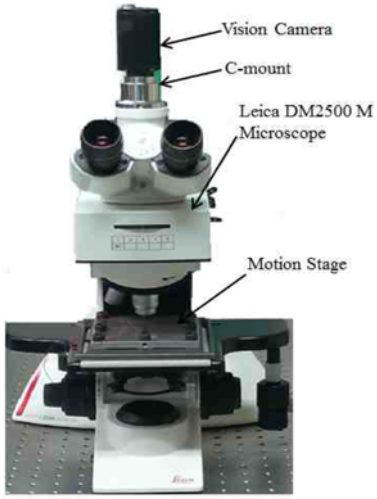

Fig. 11 Microscope for motion stage measurement

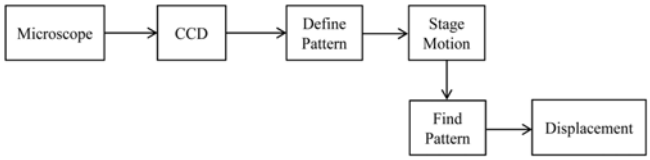

Fig. 12 Measurement block diagram

captured using a CCD camera attached to the microscope via a C-mount adapter. The camera is connected to a PC that has a frame grabber installed. A Labview software program is implemented to measure the in-plane x-y motion of the motion stage using pattern matching method. A block diagram of the measurement process is shown in Fig. 12. The pattern matching process consists of defining a pattern of the object that is moving, in our case the motion stage, and then finding that pattern, i.e., object, in each image grabbed by the CCD to estimate the

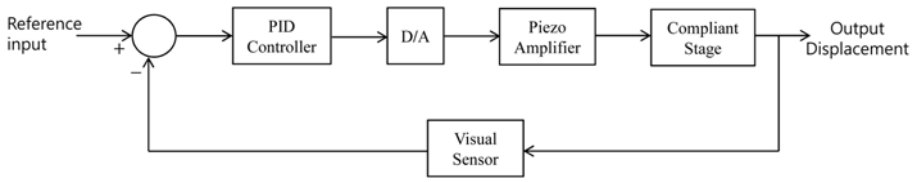

Fig. 13 Block diagram of the PID control

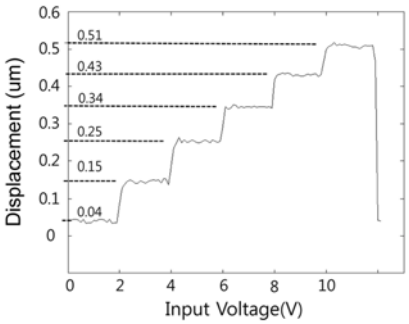

Fig. 14 Piezo displacement

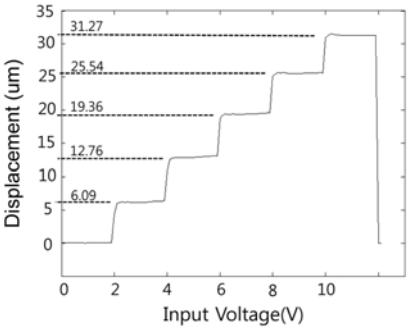

Fig. 15 Motion stage displacement

motion of that object.

An image model $M_i(x, y)$ is defined for each of the targets. Each of these targets is matched in real time against the incoming images $I(x, y)$.

$$r(u,v)=\frac{\Sigma I(x,y)M_i(x-u,y-v)-\bar{I}\cdot\overline{M}_i}{\sqrt{[I(x,y)^2-\bar{I}^2]\cdot[\Sigma M_i(x-u,y-v)^2-\overline{M}_i^2]}} \quad (11)$$

where $\overline{M_i}$ is the mean of the model i and $\bar{I}$ is the mean of $I(x, y)$. Thus,

$$r(\hat{x}_i,\hat{y}_i)=\max\{r(u,v)\} \quad (12)$$

$r(\hat{x}_i,\hat{y}_i)$ represents the position of the estimated position of the object. The frame grabber has a frame rate of 30 Hz determining the sampling rate of the sensor.

3.3 Motion stage displacement

In order to verify the amplification ratio of the motion stage, motion of the piezo element (Fig. 14) and the motion end effecter (Fig. 15) has been measured. The same voltage has been applied to the piezo element in each case. Table 4 presents the measurement results along with the amplification ratio. The average amplification ratio exceeds 60. This is smaller than the simulation result of 70, however a very large amplification ratio compared to previously reported designs.

Table 4 Experimental result

Voltage (V)	Piezo displacement (um)	Motion stage displacement (um)	Amplification ratio
2	0.11	6.09	53.36
4	0.21	12.76	60.76
6	0.3	19.36	64.53
8	0.39	25.54	65.49
10	0.47	31.27	66.53

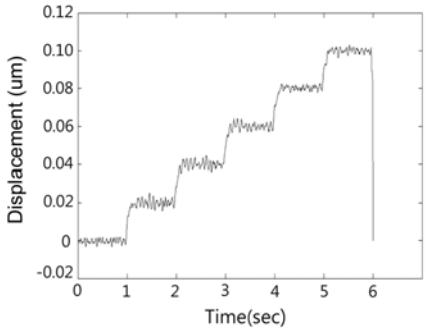

Fig. 16 20 nm step resolution

3.4 Motion stage control

To verify the performance of the motion stage a simple closed loop motion control scheme has been devised based on measurements of the motion stage. The block diagram based on a simple proportional-integral-derivative (PID) controller of the system is shown in Fig. 13. The visual measurement system is directly integrated with the stage for real time motion measurement. The reference input is compared with the measured motion, and the error signal is used for the PID controller.

20 nm step inputs were performed to evaluate the performance of the close-loop system and are shown in Fig. 15. The sampling rate of the feedback is 30 Hz which is limited by the CCD frame rate. The nano-stepping results indicate that the resolution of the motion stage is better than 10 nm. The apparent noise envelope shown in Fig. 15 is due to the vibration of the overall structure. It appears that perhaps better results can be obtained if better vibration isolation of the entire motion stage instrumentation can be done.

4. Conclusions

This paper presents a novel piezo driven motion stage employing multiple motion levers allowing for an amplification ratio that exceeds

60x enabled by a newly contrived cross hinge structure. The motion stage was incorporated into a close loop motion control scheme capable of 20 nm nano-stepping. Optimization of the motion stage was performed and simulation results proved the superiority of the newly devised cross hinge compared to the conventional flexure hinge. Upon further end-effector design for the motion stage, the developed system can be possibly integrated into high precision applications. Furthermore, the cross-hinge design can be adapted into previous designs to enhance performance.

ACKNOWLEDGEMENT

This research was supported by Kyungsung University Research Grants in 2014.

REFERENCES

1. Scire, F. E. and Teague, E. C., "Piezodriven 50-μm Range Stage with Subnanometer Resolution," Review of Scientific Instruments, Vol. 49, No. 12, pp. 1735-1740, 1978.
2. Choi, S. B., Han, S. S., and Lee, Y. S., "Fine Motion Control of a Moving Stage using a Piezoactuator Associated with a Displacement Amplifier," Smart Materials and Structures, Vol. 14, No. 1, pp. 222-230, 2005.
3. Kang, B. H., Ting-Yung Wen, J., Dagalakis, N. G., and Gorman, J. J., "Analysis and Design of Parallel Mechanisms with Flexure Joints," IEEE Transactions on Robotics, Vol. 21, No. 6, pp. 1179-1185, 2005.
4. Gao, P., Swei, S.-M., and Yuan, Z., "A New Piezodriven Precision Micropositioning Stage Utilizing Flexure Hinges," Nanotechnology, Vol. 10, No. 4, pp. 394-398, 1999.
5. Lu, T. F., Handley, D. C., Yong, Y. K., and Eales, C., "A Three-Dof Compliant Micromotion Stage with Flexure Hinges," Industrial Robot: An International Journal, Vol. 31, No. 4, pp. 355-361, 2004.
6. Ryu, J. W., Gweon, D.-G., and Moon, K. S., "Optimal Design of a Flexure Hinge based XYφ Wafer Stage," Precision Engineering, Vol. 21, No. 1, pp. 18-28, 1997.
7. Hu, K., Kim, J. H., Schmiedeler, J., and Menq, C. H., "Design, Implementation, and Control of a Six-Axis Compliant Stage," Review of Scientific Instruments, Vol. 79, No. 2, Paper No. 025105, 2008.
8. Jae, W. S., "A Study on the Displacement Magnification Mechanism of Ultraprecision stage Using Linear Lever," M.Sc. Thesis, Department of Mechanical Engineering, Dong Eui University, 2008.
9. Hwang, E. J., Min, K. S., Song, S. H., Ahn, I. H., and Choi, W. C., "Optimal Design of a Flexure-Hinge Precision Stage with a Lever," Journal of Mechanical Science and Technology, Vol. 21, No. 4, pp. 616-623, 2007.
10. Hwang, D. H., Park, J. H., Jeong, J. W., Lee, M. G., "Optima Design of a Flexure Guided Stage with Piezo Electric Transducers," Proc. of KSPE Spring Conference, pp. 397-398, 2008.
11. Kim, J. Y., Kwac, L. K., Han, J. H., Kim, H. W., and Shimokohbe, A., "A Study on the Optimal Structural Design using FEM for Micro Stage," J. Korean Soc. Precis. Eng., Vol. 19, No. 10, pp. 60-65, 2002.
12. Choi, K. B., Lee, J. J., Kim, M. Y., and Ko, K. W., "Analysis of a Rotation Stage with Cartwheel-Type Flexure Hinges Driven by a Stack-Type Piezoelectric Element," J. Korean Soc. Precis. Eng., Vol. 24, No. 12, pp. 1225-9071, 2007.
13. Shin, D. I., Kim, Y. S., Shu, S. W., Han, C., Choi, D. S., and Whang, K. H., "Development of 3-DOF Parallel Manipulator Using Flexure Hinge," J. Korean Soc. Precis. Eng., Vol. 26, No. 7, pp. 127-133, 2009.